ChemSystemsChem

Research Article
doi.org/10.1002/syst.202200034

Chemistry Europe
European Chemical Societies Publishing

www.chemsystemschem.org

Special Collection

Iron-Mediated Peptide Formation in Water and Liquid Sulfur Dioxide under Prebiotically Plausible Conditions**

Constanze Sydow[+],[a] Fabian Sauer[+],[a] Alexander F. Siegle,[a] and Oliver Trapp*[a, b]

Peptides have essential structural and catalytic functions in living organisms. The formation of peptides requires the overcoming of thermodynamic and kinetic barriers. In recent years, various formation scenarios that may have occurred during the origin of life have been investigated, including iron(III)-catalyzed condensations. However, iron(III)-catalysts require elevated temperatures and the catalytic activity in peptide bond forming reactions is often low. It is likely that in an anoxic environment such as that of the early Earth, reduced iron compounds were abundant, both on the Earth's surface itself and as a major component of iron meteorites. In this work, we show that reduced iron activated by acetic acid mediates efficiently peptide formation. We recently demonstrated that, compared to water, liquid sulfur dioxide (SO_2) is a superior reaction medium for peptide formations. We thus investigated both and observed up to four amino acid/peptide coupling steps in each solvent. Reaction with diglycine (G_2) formed 2.0% triglycine (G_3) and 7.6% tetraglycine (G_4) in 21 d. Addition of G_3 and dialanine (A_2) yielded 8.7% G_4. Therefore, this is an efficient and plausible route for the formation of the first peptides as simple catalysts for further transformations in such environments.

Introduction

In living organisms, peptides fulfill various essential functions, such as cellular signaling, structural tasks or catalysis, making them indispensable everywhere in nature.[1] Consequently, their formation paths at the very beginning of the origin of life are of great interest. As generally accepted, the required condensation of amino acids is thermodynamically and kinetically unfavorable in aqueous solutions. To overcome this obstacle several scenarios for the emergence of peptides have been proposed, involving the presence of condensation agents and activated amino acid derivatives,[2] dry heating,[3] mechanochemical reaction conditions and non-aqueous reaction media,[4] such as eutectic and sulfur dioxide (SO_2) solutions.[4b,5] Metal and mineral catalysis under conditions that promote dehydration is another strategy to circumvent the constraints in aqueous solution.[6] Although some remarkable peptide yields were obtained from these routes, the availability of frequently required condensation agents such as polyphosphates, imidazole, cyanates and cyanamides in sufficient concentrations on the early Earth is still controversial.[6c,7] Prebiotic peptide syntheses should be based on easily available reagents to ensure their compatibility with various scenarios. Iron as a highly abundant element on (early) Earth perfectly meets this requirement.[8] Assuming an atmosphere that mainly consisted of N_2 and CO_2 with traces of CO, H_2 and reduced sulfur gases, i.e., an anoxic environment,[9] makes the coexistence of iron(III)-minerals and reduced iron compounds plausible.[8a,10] A weakly reducing atmosphere stabilizes elemental iron derived from meteorite impacts or serpentinization of mafic rocks and iron(II)-minerals stemming from weathering of the basalt- and komatiite-rich earth crust in the Hadean eon.[8a,11] Previous studies focused mainly on iron(III)-mediated peptide formation.[12] With the environmental constraints of an anoxic environment in mind we propose that reduced iron species might be superior mediators for prebiotic peptide syntheses. However, to our knowledge, neither metallic iron as starting material nor active iron(II)-intermediates have yet been considered for prebiotic amino acid coupling. Up to date the role of iron(II) in peptide syntheses is limited to an additive and surface material in COS or CO and H_2S activated amino acid coupling by Ghadiri and Wächtershäuser.[2b,13] Thus, we intended to exploit the potential of reduced iron and iron compounds as coupling agents in an effective peptide synthesis starting from prebiotically plausible reactants (Figure 1a),[14] because the corrosion of iron supports the necessary dehydration in the peptide coupling and brings the amino acids into close proximity through coordination.

[a] C. Sydow,[+] Dr. F. Sauer,[+] Dr. A. F. Siegle, Prof. Dr. O. Trapp
Department of Chemistry
Ludwig Maximilians University Munich
Butenandtstraße 5–13, 81377 Munich (Germany)
E-mail: oliver.trapp@cup.uni.muenchen.de
[b] Prof. Dr. O. Trapp
Max-Planck-Institute for Astronomy
Königstuhl 17, 69117 Heidelberg (Germany)

[+] These authors contributed equally to this work.

[**] A previous version of this manuscript has been deposited on a preprint server (https://doi.org/10.26434/chemrxiv-2022-gr80t).

Supporting information for this article is available on the WWW under https://doi.org/10.1002/syst.202200034

Special Collection An invited contribution to a Special Collection on Protocells and Prebiotic Systems.

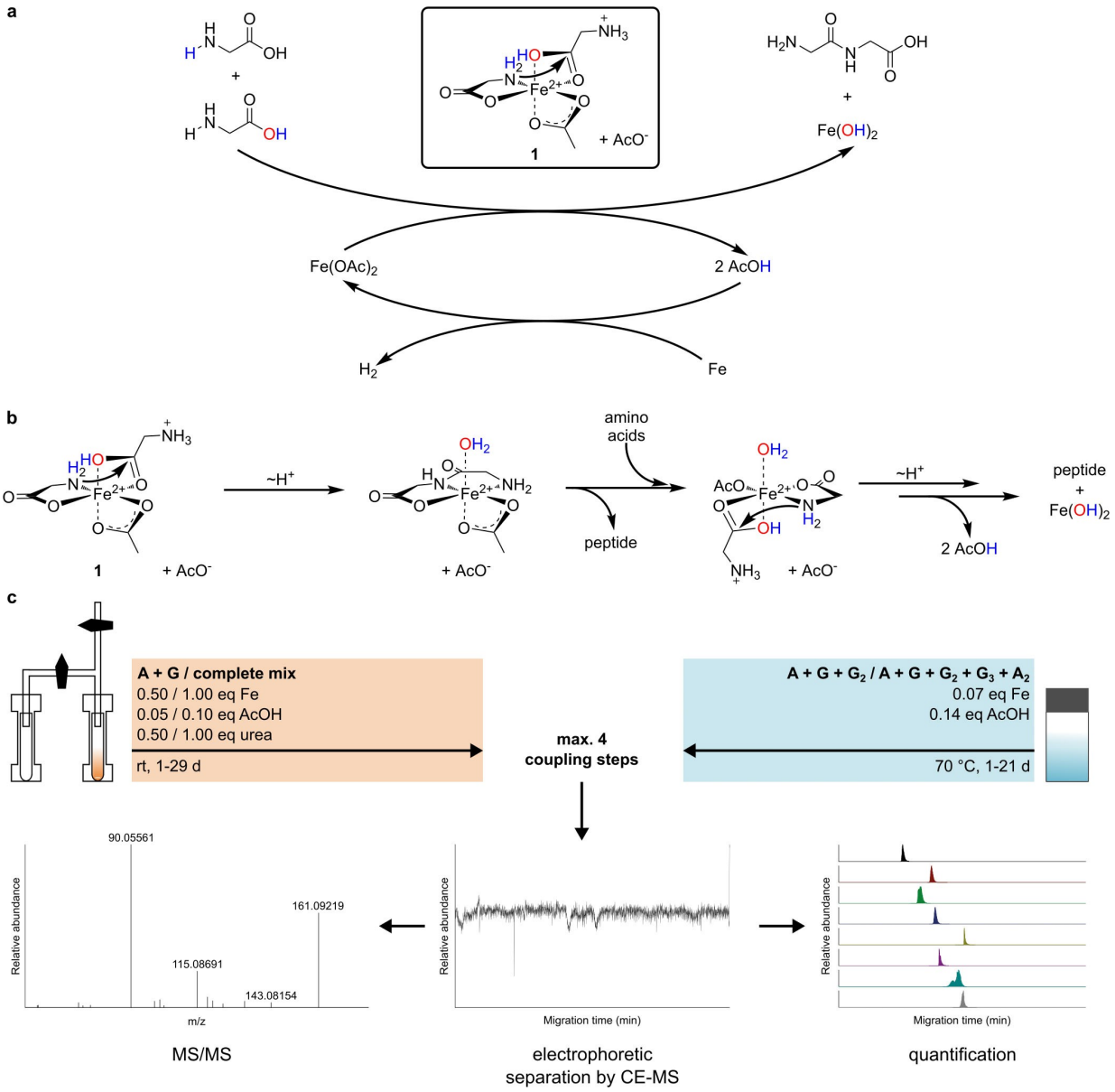

Figure 1. Proposed mechanism exemplified for the coupling of amino acids and experimental workflow. a) Proposed reaction cycle of the iron-mediated peptide formation, including $Fe(OAc)_2$ formation, amino acid coupling and AcOH regeneration. b) Proposed mechanism for the amino acid coupling (see also Scheme S1). c) Experimental setup: reactions in liquid SO_2 were performed at room temperature in a pressure apparatus, reactions in H_2O at 70 °C. Product analysis was performed by CE-MS measurements.

Results and Discussion

Initial corrosion of elemental iron is promoted by acetic acid (AcOH). The formation of carboxylic acids and in particular of AcOH under primordial conditions is well known.[14a,15] We propose that formation of iron(II)-species ($Fe(OAc)_2$) and coordination of amino acids/peptides lead to an iron(II)-complex mediated coupling step (exemplified for the coupling of amino acids: Figure 1a and b, Scheme S1).

The intermediate of the peptide formation is proposed to be a distorted octahedral complex **1** as iron(II) amino acid complexes and $Fe(OAc)_2$ are distorted high-spin (HS) complexes.[16] This structural characteristic supports the removal of water emerging from the coupling step from the reaction site, regenerating AcOH after a second condensation step. We further propose that water is efficiently removed from the reaction cycle by formation of iron hydroxide, which is the thermodynamic driving force of the reaction. In the next reaction cycle regenerated AcOH reacts with elemental iron from the reservoir, again providing iron(II)-precursors for further amino acid couplings.

We recently demonstrated for copper-mediated peptide coupling, that in an environment of liquid SO_2 already lower amino acid and copper loadings yielded greater amounts of products under milder reaction conditions.[5] Therefore, we investigated the iron-mediated peptide synthesis in water and

liquid SO_2 by reaction of iron powder, amino acids, AcOH and urea as an additive. Product mixtures were separated and analyzed by capillary electrophoresis coupled to electrospray Orbitrap mass spectrometry (CE-MS).[17] Formed peptides were quantified and sequence analysis was performed by tandem mass spectrometry (MS/MS) (Figure 1c).

First, the reaction conditions for iron-mediated peptide formation in water were screened using alanine (A), glycine (G), and diglycine (G_2) as starting materials. The reaction temperature and the reactant ratios were systematically varied. In addition, the influence of urea which is known as promoter in prebiotic peptide bond formation and phosphorylation was investigated.[5,14b,18]

Interestingly, peptide formation could be also observed in absence of AcOH. G-containing peptides up to G_4 could be detected, implying that either amino acids themselves oxidize the elemental iron or elemental iron is capable to mediate the peptide formation (Figures S15 and 16). However, small traces of AcOH (0.07 eq, based on the total amount of amino acid) significantly accelerated the corrosion of the iron powder, resulting in an enhanced peptide yield (Figures S2 and S17–22). In the presence of larger amounts of AcOH amino acid coupling was still observed, however conversion decreased slightly. The more acidic conditions cause increased peptide cleavage.[19] Both large excesses (3.00 eq) as well as traces of iron led to efficient peptide synthesis and even 0.01 eq iron powder produced various di- to hexapeptides (Figures S3, S23–40). Maximum peptide formation and a homogenous reaction mixture were observed with 6.67 eq water. Both further dilution and reduced water quantities led to decreased product formation (Figure S4, S41–66).

Furthermore, the influence of urea as an additive was investigated; its yield-increasing influence on metal-catalyzed dipeptide syntheses has already been described.[5] Urea enhances the conversion by improving the solubility of the peptides and can remove water upon decomposition.[20] For our screening 0.50 or 1.00 eq urea was added to the reaction mixture (Figures S5 and S67–86). We found that the influence of urea on the reaction depends on the specific peptide. With increasing urea concentration, the conversion of A-containing peptides increases, but at the same time the yield of G-containing peptides decreases. This effect increases with the length of the peptide chains, which is caused by suppressing stabilizing intramolecular interactions of the peptide by urea,[20] limiting the synthesis of longer oligomers.

In the presence of iron(II) acetate $Fe(OAc)_2$ peptide coupling can be observed, corroborating that an iron(II)-complex mediates the coupling reaction (Figure 1a and b, Table 1, Figures S87–94).

Traces of G_3 and G_4 were detected after 21 days (d) at room temperature (Figures S95 and 96). Higher temperatures accelerated the reaction, so that G_7 could be detected at 70 °C already after 7 d (Figures S97 and 98). However, at the same time elevated temperatures enabled side product formation. In analogy to iron(III)-catalyzed condensations the G based cyclic dipeptide product (diketopiperazine) was obtained in 1% yield referred to G_2. Furthermore, acetylated reactants were observed (Figures S99, 100). Overall, the iron-mediated peptide synthesis proceeds over a wide range of reaction conditions. Peptide traces are detected under mild reaction conditions.

Next, we investigated the reaction progress of the iron-mediated peptide synthesis in water at 70 °C, for which the peptide yields of the reaction were determined after 1, 3, 7, and 21 d (Table 1, Figures S6–8, S101–144, S261–264, Tables S1, S4–7). Di- to tetrapeptides were detected after only 1 d, including AG, AG_2, A_2G, G_3, and G_4 (and the corresponding inverse sequences), and over the course of 21 d both the yields and the number of peptide products increased steadily. A_2 was formed after 3 d, and after 21 d G_9 was detected as the longest polypeptide. G_3 and G_4 were synthesized within 21 d with a yield of 2.0 and 7.6%. Adding peptides G_3 and A_2 to the reaction mixture resulted in increased yields of longer oligomers (Table 1, Figures S145–180, Tables S1, S8–10). G_4 was synthesized within 21 d with a yield of 8.7%, G_{10} was detected as the longest peptide chain. Within 21 d, the yield of each peptide product increased, confirming that longer reaction times not only lead to better yields but also result in longer oligomers. It is important to note that peptide hydrolysis was not observed under these conditions, which agrees very well with kinetic studies.[21]

Based on these results, peptide synthesis by iron-mediated amino acid coupling in aqueous medium is a very promising and prebiotically plausible route. In view of the results of our previous studies for peptide synthesis in liquid SO_2, we intended to test the applicability of the route to another scenario and transferred the iron-mediated synthesis to this solvent.[5] However, initial experiments with 0.50 eq of iron powder (based on the total amount of amino acids) and an amino acid mixture of G and A with 0.05 eq of AcOH in SO_2 at room temperature for 7 d resulted in the formation of only trace amounts of G_2 (Figures S9, S181–183).

In analogy to the reaction in water, the influence of urea on peptide formation in SO_2 was investigated. The addition of 0.25 eq urea led to the formation of all possible dipeptide combinations and 0.50 eq even allowed the formation of tripeptides after 7 d (Figures S9, S184–189, Table S3), consequently 0.50 eq urea was used in all subsequent reactions.

Based on the optimized reaction conditions, we investigated the applicability of the proposed mechanism to the reaction in SO_2 (Figure 1a and b). When AcOH is regenerated, catalytic amounts of AcOH should be sufficient for peptide synthesis. An investigation of peptide yield as a function of AcOH concentration showed a maximum at 0.05 eq (Table 2, Figures S10, S187–198, S265–278, Tables S3, S11–16). In analogy to the synthesis in aqueous medium, an increasing AcOH concentration leads to peptide cleavage and decrease in yield.[19] Interestingly, dipeptides were observed after 7 d even without addition of AcOH. In addition to the reasons discussed for the reaction in aqueous solution, oxidation of elemental iron by SO_2 itself must be considered.[22] Product formation without accelerated corrosion by AcOH and even at low concentrations is particularly interesting from a prebiotic perspective, as many scenarios for the emergence of life assume low reactant concentrations. Screening of various iron concentrations

Table 1. Overview of reaction conditions, coupling steps, products and yields for the iron-mediated peptide formation in H_2O. Products in brackets refer to the entirety of all inverse sequences. Yields were determined by CE-MS measurements. Error bars indicate ± s.d. obtained from two experiments by double determination via CE-MS.

reactants	c per reactant [M]	iron species	AcOH [eq]	t [d]	max. number of coupling steps starting from G_2	products	Yield [%]
A, G, G2	2.61	0.07 eq Fe	0.14	1	1	(AG)	traces[a]
						G_3	0.14 ± 0.03
						G_4	0.17 ± 0.03
						(AG_2), (A_2G)	n.d.[b]
A, G, G2	2.61	0.07 eq Fe	0.14	3	1	(AG)	0.02 ± 0.00
						G_3	0.37 ± 0.05
						G_4	0.61 ± 0.14
						A_2	traces[a]
						(AG_2), (A_2G), G_5	n.d.[b]
A, G, G2	2.61	0.07 eq Fe	0.14	7	2	(AG)	0.05 ± 0.00
						G_3	0.93 ± 0.05
						G_4	3.26 ± 0.15
						A_2	traces[a]
						(AG_2), (A_2G), G_5, G_6	n.d.[b]
A, G, G2	2.61	0.07 eq Fe	0.14	21	3	(AG)	0.15 ± 0.02
						G_3	2.03 ± 0.22
						G_4	7.56 ± 0.39
						A_2	traces[a]
						(AG_2), (A_2G), (A_2G_2), G_5, G_6, G_7, G_8, G_9	n.d.[b]
							n.d.[b]
A, G, G2	2.31	0.07 eq $Fe(OAc)_2$	–	7		(AG), G_3, G_4, A_2, (AG_2), (A_2G), G_5, Gs	n.d.[b]
							n.d.[b]
A, G, G2, A2, G3	1.57	0.07 eq Fe	0.14	7	3	(AG)	0.06 ± 0.01
						A_3	0.06 ± 0.01
						G_4	5.57 ± 0.34
						(AG_2), (A_2G), A_4, (A_2G_2), G_5, G_6, G_7, G_8, G_9	n.d.[b]
							n.d.[b]
A, G, G2, A2, G3	1.57	0.07 eq Fe	0.14	14	4	(AG)	0.14 ± 0.01
						A_3	0.07 ± 0.01
						G_4	7.83 ± 1.08
						(AG_2), (A_2G), A_4, (A_2G_2), G_5, G_6, G_7, G_8, G_9, G_{10}	n.d.[b]
							n.d.[b]
A, G, G2, A2, G3	1.57	0.07 eq Fe	0.14	21	4	(AG)	0.23 ± 0.02
						A_3	0.09 ± 0.00
						G_4	8.66 ± 0.43
						(AG_2), (A_2G), A_4, (A_2G_2), G_5, G_6, G_7, G_8, G_9, G_{10}	n.d.[b]
							n.d.[b]

[a] Yield too low for quantification. [b] Not determined

showed that higher yields and broader product ranges could be observed for higher metal concentrations (Table 2, Figures S11, S187–189, S199–207, S273 and 274, S279–283, Tables S3, S11 and 12, S17–20). Despite that, traces of G_2 form even without the addition of elemental iron and iron quantities as small as 0.05 eq yielded 0.3% G_2 and even enabled the formation of tripeptides.

As in the aqueous reaction, the substitution of elemental iron and AcOH by $Fe(OAc)_2$ (0.05 eq) yields peptides corroborating that an iron(II)-complex mediates the coupling reaction. With $Fe(OAc)_2$ di- and tripeptides formed after 7 d (Table 2, Figures S12, S208–210, S284–286, Tables S3, S21 and 22).

Starting from the optimized conditions including elemental iron (0.50 eq), catalytic AcOH quantities (0.05 eq) and the addition of urea (0.50 eq), we investigated the reaction time dependence of the peptide yields for the A, G system (Table 2, Figures S13, 14, S187–189, S214–228, S273–274, S289–291, Tables S2 and 3, S11 and 12, S25 and 26). G_2 and GA already formed after 1 d and their yields increased continuously over time, resulting in 2.5% G_2 and 1.4% AG/GA after 29 d. After 3 d A_2 and traces of G_3 and after 7 d G_2A could be detected. In addition to that, the iron-mediated reaction in SO_2 yielded tetra- and even various pentapeptides after 29 d. Diketopiperazines and acetylated amino acids were absent in liquid SO_2.

Replacing iron powder with the Hadean mineral marcasite (FeS_2) also led to peptide formation, further corroborating the prebiotic plausibility of the presented synthetic pathway.[8a] The conversion of A and G with the mineral and urea for 7 d yielded G_2, GA, A_2 and even G_3 and AG_2 in trace amounts (tripeptide sequences could not be identified) (Table 2, Figures S12, S229-231, S284, S287 and 288, Tables S3, S23 and 24).

Furthermore, we tested G_2 as reactant in liquid SO_2. Starting with G and G_2 in the presence of iron, urea (each 0.50 eq) and AcOH (0.05 eq) we observed up to two condensation steps and the formation of G_3 to G_6 (Figures S211–213).

To investigate the performance of the reaction in a more complex system, we applied iron-mediated peptide synthesis in liquid SO_2 to a larger amino acid mixture consisting of all 20 proteinogenic amino acids. The resulting peptide mixture was separated by capillary electrophoresis and the dipeptide

Table 2. Overview of reaction conditions, coupling steps, products and yields for the iron-mediated peptide formation in SO_2 starting from A and G (each 400 mM, in total 1.00 eq). Products in brackets refer to the entirety of all inverse sequences. Yields were determined by CE measurements. Error bars indicate ±s.d. obtained by double determination via CE. Sequences which could be determined unambiguously by MS/MS are depicted in Table S3.

iron species	AcOH [eq]	Urea [eq]	t [d]	max. number of coupling steps	products	Yield [%]
0.50 eq Fe	0.05	0.50	1	1	G_2, (AG)	traces[a]
0.50 eq Fe	0.05	0.50	3	2	G_2, (AG), A_2	traces[a, b]
					G_3	n.d.[c]
0.50 eq Fe	0.05	0.50	7	2	G_2	0.54 ± 0.02
					(AG)	0.13 ± 0.02
					A_2	traces[b]
					G_3, (AG_2)	n.d.[c]
0.50 eq Fe	0.05	0.50	29	4	G_2	2.48 ± 0.45
					(AG)	1.38 ± 0.22
					A_2	1.48 ± 0.21
					G_3, (AG_2), (A_2G), A_3,	n.d.[c]
					G_4, A_4, (AG_3), (A_2G_2),	n.d.[c]
					(A_3G), G_5, (AG_4),	
					(A_2G_3), (A_3G_2)	
0.50 eq Fe	0.25	0.50	7	2	G_2	0.33 ± 0.04
					(AG)	0.11 ± 0.01
					A_2	traces[b]
					G_3, (AG_2)	n.d.[c]
0.50 eq Fe	0.50	0.50	7	2	G_2	0.25 ± 0.06
					(AG)	0.09 ± 0.01
					A_2	traces[b]
					G_3, (AG_2)	n.d.[c]
0.05 eq $Fe(OAc)_2$	–	0.50	7	2	G_2	0.35 ± 0.02
					(AG)	0.16 ± 0.01
					A_2	traces[b]
					G_3, (AG_2)	n.d.[c]
0.05 eq Fe	0.05	0.50	7	2	G_2	0.29 ± 0.13
					(AG)	0.10 ± 0.02
					A_2	traces[b]
					G_3, (AG_2)	n.d.[c]
0.25 eq Fe	0.05	0.50	7	2	G_2	0.46 ± 0.04
					(AG)	0.15 ± 0.01
					A_2	traces[b]
					G_3, (AG_2)	n.d.[c]
20.9 mmol/g FeS_2	–	0.50	7	2	G_2	0.17 ± 0.01
					(AG), A_2	traces[a,b]
					G_3, (AG_2)	n.d.[c]

[a] Yield too low for quantification. [b] Insufficient electrophoretic separation of A_2 and monomer prevented A_2 quantification. [c] Not determined.

sequences were identified by MS/MS experiments (Figure 2, Figures S232–260). Incorporation of all amino acids into dipeptides emphasizes the versatility of the synthetic pathway. Alkaline amino acids exhibited outstanding conversion to dipeptides, whereas the inferior reactivity of acidic amino acids and tyrosine (Y) might be a result of their low solubility.[5] Also remarkable is the formation of various proline (P) based peptides, which are known to be catalytically active.[23]

Conclusion

In summary, peptide formation by reduced iron from prebiotically available reactants at room temperature led to quantifiable dipeptide amounts in SO_2 and to peptide traces in aqueous solution. The aqueous reaction showed increased peptide formation at 70 °C, though at elevated temperatures diketopiperazines and acetylated side products were obtained. Furthermore, up to four condensations steps per peptide chain were accomplished in SO_2 even at room temperature and in water at 70 °C which could not be observed in previous iron(III)-mediated peptide formation.[12] Comparison of the presented route with the iron(III)-pathways showed that products accessible via the same number of coupling steps are able to compete in yield. The incorporation of all proteinogenic amino acids into peptides and the successful substitution of iron powder with the Hadean mineral marcasite corroborate the applicability of the peptide formation by reduced iron to complex scenarios related to the origin of life. The presented synthetic pathway is compatible with a wide range of prebiotically plausible scenarios as a result of the high iron abundance.[8a] Even iron containing meteorites are conceivable reaction sites for iron-mediated peptide formation.

Experimental Section

Peptide condensation in water. An amino acid mixture of equimolar parts of l-alanine (A), glycine (G) and diglycine (G_2) (800 mg, 8.10 mmol in total, 1.00 eq) was mixed with iron powder (30.2 mg, 0.54 mmol, 0.07 eq) and added to a 4 mL glass vial. Acetic acid

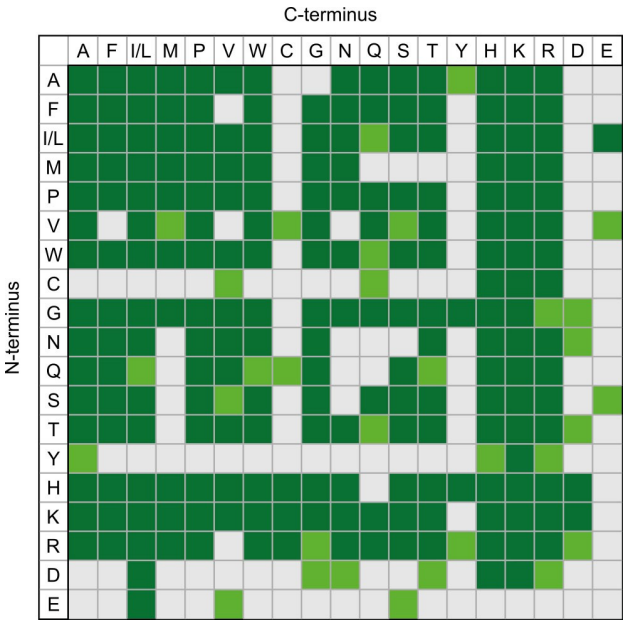

Figure 2. Product spectrum of the complete amino acid mixture in SO_2. Dipeptides detected from the reaction of all 20 proteinogenic amino acids (in total 400 mM, 1.00 eq) with iron powder, urea (each 1.00 eq) and AcOH (0.10 eq) in SO_2 after 7 d (dark green = confirmed by MS/MS, light green = traces detected, white = not detected).

(AcOH) (61.8 µL, 1.08 mmol, 0.14 eq) and H_2O (973 µL, 54.0 mmol, 6.67 eq) were added. The vials were sealed and transferred to a metal block at 70 °C on a shaking plate. Unless otherwise stated, samples were taken after 1, 3, 7 and 21 d. All experiments were repeated twice and each analyzed twice.

Peptide condensation in liquid SO_2. G (90.1 mg, 1.20 mmol), L-A (106.9 mg, 1.20 mmol) (2.40 mmol in total, 1.00 eq), urea (72.1 mg, 1.20 mmol, 0.50 eq) and iron powder (67.2 mg, 1.20 mmol, 0.50 eq) or optionally either marcasite (FeS_2) (114.8 mg, amino acid/mineral ratio of 20.9 mmol/g) or $Fe(OAc)_2$ (20.9 mg, 120 µmol, 0.05 eq) were mixed. For the reaction of the complete amino acid mixture (1.20 mmol in total, 1.00 eq) in the presence of urea (72.1 mg, 1.20 mmol, 1.00 eq) iron powder (67.2 mg, 1.20 mmol, 1.00 eq) was used as starting material. When using iron powder the reaction mixture was incubated with AcOH (6.90 µL, 120 µmol) for 2 h. The glass tube was inserted into the stainless steel apparatus on the reaction side (Figure S1). The reaction mixture was evacuated and flushed with nitrogen three times. SO_2 (3 mL) from the storage chamber was condensed on to the reaction mixture at −76 °C. The resulting pressure in the chamber is 3.2 bar. The reaction mixture was stirred for 1 to 29 d at room temperature. At the end of the reaction time SO_2 was condensed back into the storage chamber to be reused for up to four more reactions. The solid residue was dried *in vacuo* and stored at -50 °C.

CE-MS/MS analysis. Prior to analysis all samples were diluted and filtered through a syringe filter (cellulose acetate, pore size 0.45 µm). Samples containing A and G were diluted to 5 mM and the sample containing the complete amino acid mixture to 1 mM referring to the initial concentration of one amino acid. Peptide analysis was performed on an Agilent 7100 CE System coupled to a Thermo Scientific Q Exactive Plus mass spectrometer using a home-built sheath-flow interface, which is described elsewhere.[17] Electrophoretic separations in positive polarity mode were conducted at 25 °C by applying 30 kV to the CE inlet. In addition, a constant pressure of 30 mbar was applied to accelerate the analyses. Prior to analysis bare fused silica capillaries (ID = 50 µm, l = 80 cm) were coated with linear polyacrylamide to avoid peptide adsorption on the capillary wall. The polyimide coating at the outer capillary wall was removed at the MS end. The coating procedure is described elsewhere.[5] Aqueous AcOH (2 M) was used as background electrolyte (BGE). New capillaries were conditioned with deionized water, aqueous H_3PO_4 (10 mM), deionized water and BGE (each 5 min). Further conditioning between measurement runs with deionized water, H_3PO_4 (10 mM), deionized water (each 2 min) and BGE (2 M) (3 min) ensured proper analyses. Samples were injected by applying 30 mbar for 10 s to the CE inlet. During analyses, the application of an external voltage (3.2 kV) to the stainless steel emitter and a sheath liquid flow (isopropanol (IPA)/deionized water 1:1 with 0.05 % formic acid (FA); flow rate 3 µL/min) ensured a stable electrospray.

Mass spectrometer settings were adjusted to 140 °C for the ion transfer capillary temperature and to 50 for the S-lens RF level. Full Scan (m/z 122–750 and for the detection of side products m/z 50–750) mass spectra were collected at a resolution of 70000. Data dependent MS/MS analysis based on inclusion lists covering all possible peptide combinations was conducted to determine the dipeptide sequences. Peptide fragmentation was performed by applying a normalized collision energy of 30 %. The resolution of the MS/MS spectra was set to 17500. Thermo Xcalibur software 4.1 was used to evaluate the mass spectra.

CE analysis. Prior to analysis samples were diluted to 10 mM referring to the initial concentration of one amino acid. Dipeptide quantification was performed on bare fused silica capillaries with a total length of 80 cm and aqueous AcOH (2 M) as BGE using an Agilent 7100 CE system equipped with a conductivity detector. Sample injection was accomplished by applying 30 mbar for 10 s. Peptides were separated in positive polarity mode at 25 °C by applying 30 kV to the CE inlet. 4-hydroxyproline (4-HP) (100 µM) was added as internal standard and calibration runs of a standard mixture containing G_2, (alanyl)glycine (AG) + (glycyl)alanine (GA) and (alanyl)alanine (A_2) were performed in triplicates. New capillaries were flushed with deionized water, aqueous NaOH (0.1 M), deionized water and BGE (each 5 min) prior to the first analysis. Between analysis runs capillaries were conditioned with deionized water, aqueous NaOH (0.1 M), deionized water (each 2 min) and BGE (3 min). CEval 0.6 g and OriginPro 2018G were used to evaluate the CE electropherograms.[24]

Acknowledgements

We acknowledge financial support from the Ludwig-Maximilians-University Munich, the Max-Planck-Society (Max-Planck-Fellow Research Group Origins of Life), the Volkswagen Stiftung (Initiating Molecular Life), the Deutsche Forschungsgemeinschaft DFG/German Research Foundation (Project-ID 364653263 – TRR 235, Emergence of Life) and Germany's Excellence Strategy (ORIGINS, EXC-2094 – 390783311). Open Access funding enabled and organized by Projekt DEAL.

Conflict of Interest

The authors declare no conflict of interest.

Data Availability Statement

The data that support the findings of this study are available in the supplementary material of this article.

Keywords: amino acids · iron · origin of life · peptides · prebiotic chemistry

[1] M. Frenkel-Pinter, *Chem. Rev.* **2020**, *120*, 4707–4765.
[2] a) E. T. Parker, M. Zhou, A. S. Burton, D. P. Glavin, J. P. Dworkin, R. Krishnamurthy, F. M. Fernández, J. L. Bada, *Angew. Chem.* **2014**, *126*, 8270–8274; *Angew. Chem. Int. Ed.* **2014**, *53*, 8132–8136; b) L. Leman, L. Orgel, M. R. Ghadiri, *Science* **2004**, *306*, 283–286; c) C. Gibard, S. Bhowmik, M. Karki, E.-K. Kim, R. Krishnamurthy, *Nat. Chem.* **2018**, *10*, 212–217; d) P. Canavelli, S. Islam, M. W. Powner, *Nature* **2019**, *571*, 546–549; e) C. S. Foden, S. Islam, C. Fernández-García, L. Maugeri, T. D. Sheppard, M. W. Powner, *Science* **2020**, *370*, 865–869.
[3] M. Rodriguez-Garcia, A. J. Surman, G. J. T. Cooper, I. Suárez-Marina, Z. Hosni, M. P. Lee, L. Cronin, *Nat. Commun.* **2015**, *6*, 8385.
[4] a) T. Stolar, S. Grubešić, N. Cindro, E. Meštrović, K. Užarević, J. G. Hernández, *Angew. Chem.* **2021**, *133*, 12837–12841; *Angew. Chem. Int. Ed.* **2021**, *60*, 12727–12731; b) M. Gull, M. Zhou, F. M. Fernández, M. A. Pasek, *J. Mol. Evol.* **2014**, *78*, 109–117.
[5] F. Sauer, M. Haas, C. Sydow, A. F. Siegle, C. A. Lauer, O. Trapp, *Nat. Commun.* **2021**, *12*, 7182.
[6] a) J.-F. Lambert, *Orig. Life Evol. Biosph.* **2008**, *38*, 211–242; b) J. P. Ferris, A. R. Hill, R. Liu, L. E. Orgel, *Nature* **1996**, *381*, 59–61; c) T. A. E. Jakschitz, B. M. Rode, *Chem. Soc. Rev.* **2012**, *41*, 5484–5489; d) D. Doran, Y. M. Abul-Haija, L. Cronin, *Angew. Chem.* **2019**, *131*, 11375–11378; *Angew. Chem. Int. Ed.* **2019**, *58*, 11253–11256; e) S. Saetia, K. R. Liedl, A. H. Eder, B. M. Rode, *Orig. Life Evol. Biosph.* **1993**, *23*, 167–176; f) J. Bujdák, K. Faybíbová, A. Eder, Y. Yongyai, B. M. Rode, *Orig. Life Evol. Biosph.* **1995**, *25*, 431–441.
[7] a) M. A. Pasek, *Chem. Rev.* **2020**, *120*, 4690–4706; b) M. G. Schwendinger, B. M. Rode, *Anal. Sci.* **1989**, *5*, 411–414.
[8] a) R. M. Hazen, *Am. J. Sci.* **2013**, *313*, 807–843; b) L. M. Barge, *Nat. Commun.* **2018**, *9*, 5170.
[9] J. F. Kasting, *Science* **1993**, *259*, 920–926.
[10] E.-I. Ochiai, *Orig. Life* **1978**, *9*, 81–91.
[11] a) J. F. Kasting, *Orig. Life Evol. Biosph.* **1990**, *20*, 199–231; b) N. G. Holm, A. Neubeck, *Geochem. Trans.* **2009**, *10*, 9; c) A. Smirnov, D. Hausner, R. Laffers, D. R. Strongin, M. A. Schoonen, *Geochem. Trans.* **2008**, *9*, 5; d) A. Meunier, S. Petit, C. S. Cockell, A. El Albani, D. Beaufort, *Orig. Life Evol. Biosph.* **2010**, *40*, 253–272.
[12] a) G. Matrajt, D. Blanot, *Amino Acids* **2004**, *26*, 153–158; b) U. Shanker, B. Bhushan, G. Bhattacharjee, Kamaluddin, *Orig. Life Evol. Biosph.* **2012**, *42*, 31–45; c) N. Kitadai, H. Oonishi, K. Umemoto, T. Usui, K. Fukushi, S. Nakashima, *Orig. Life Evol. Biosph.* **2017**, *47*, 123–143; d) T. Georgelin, M. Akouche, M. Jaber, Y. Sakhno, L. Matheron, F. Fournier, C. Méthivier, G. Martra, J.-F. Lambert, *Eur. J. Inorg. Chem.* **2017**, *2017*, 198–211; e) J. P. T. Baú, C. E. A. Carneiro, A. C. S. Da Costa, D. F. Valezi, E. Di Mauro, E. Pilau, D. A. M. Zaia, *Orig. Life Evol. Biosph.* **2021**, *51*, 299–320.
[13] C. Huber, G. Wächtershäuser, *Science* **1998**, *281*, 670–672.
[14] a) C. Huber, G. Wächtershäuser, *Science* **1997**, *276*, 245–247; b) H. J. Cleaves, J. H. Chalmers, A. Lazcano, S. L. Miller, J. L. Bada, *Orig. Life Evol. Biosph.* **2008**, *38*, 105–115.
[15] a) K. B. Muchowska, S. J. Varma, J. Moran, *Nature* **2019**, *569*, 104–107; b) M. Preiner, K. Igarashi, K. B. Muchowska, M. Yu, S. J. Varma, K. Kleinermanns, M. K. Nobu, Y. Kamagata, H. Tüysüz, J. Moran, W. F. Martin, *Nat. Ecol. Evol.* **2020**, *4*, 534–542; c) K. B. Muchowska, S. J. Varma, J. Moran, *Chem. Rev.* **2020**, *120*, 7708–7744; d) A. Wołos, R. Roszak, A. Żądło-Dobrowolska, W. Beker, B. Mikulak-Klucznik, G. Spólnik, M. Dygas, S. Szymkuć, B. A. Grzybowski, *Science* **2020**, *369*, eaaw1955; e) S. J. Varma, K. B. Muchowska, P. Chatelain, J. Moran, *Nat. Ecol. Evol.* **2018**, *2*, 1019–1024; f) N. Kitadai, R. Nakamura, M. Yamamoto, S. Okada, W. Takahagi, Y. Nakano, Y. Takahashi, K. Takai, Y. Oono, *Commun. Chem.* **2021**, *4*, 37; g) Z. Liu, L.-F. Wu, C. L. Kufner, D. D. Sasselov, W. W. Fischer, J. D. Sutherland, *Nat. Chem.* **2021**, *13*, 1126–1132.
[16] a) B. W. Fitzsimmons, A. Hume, L. F. Larkworthy, M. H. Turnbull, A. Yavari, *Inorg. Chim. Acta* **1985**, *106*, 109–114; b) B. Weber, R. Betz, W. Bauer, S. Schlamp, *Z. Anorg. Allg. Chem.* **2011**, *637*, 102–107.
[17] F. Sauer, C. Sydow, O. Trapp, *Electrophoresis* **2020**, *41*, 1280–1286.
[18] a) B. Burcar, M. Pasek, M. Gull, B. J. Cafferty, F. Velasco, N. V. Hud, C. Menor-Salván, *Angew. Chem.* **2016**, *128*, 13443–13447; *Angew. Chem. Int. Ed.* **2016**, *55*, 13249–13253; b) M. Gull, A. Omran, T. Feng, M. A. Pasek, *Life* **2020**, *10*, 122; c) R. Lohrmann, L. E. Orgel, *Science* **1971**, *171*, 490–494.
[19] C. J. Creighton, T. T. Romoff, J. H. Bu, M. Goodman, *J. Am. Chem. Soc.* **1999**, *121*, 6786–6791.
[20] L. Hua, R. Zhou, D. Thirumalai, B. J. Berne, *Proc. Nat. Acad. Sci.* **2008**, *105*, 16928–16933.
[21] A. Radzicka, R. Wolfenden, *J. Am. Chem. Soc.* **1996**, *118*, 6105–6109.
[22] S. G. Bratsch, *J. Phys. Chem. Ref. Data* **1989**, *18*, 1–21.
[23] T. Schnitzer, M. Wiesner, P. Krattiger, J. D. Revell, H. Wennemers, *Org. Biomol. Chem.* **2017**, *15*, 5877–5881.
[24] P. Dubský, M. Ördögová, M. Malý, M. Riesová, *J. Chromatogr. A* **2016**, *1445*, 158–165.

Manuscript received: September 14, 2022
Accepted manuscript online: October 17, 2022
Version of record online: November 15, 2022